JOURNAL OF VIROLOGY, Nov. 2011, p. 11557–11566 Vol. 85, No. 22
0022-538X/11/$12.00 doi:10.1128/JVI.05519-11

The Interferon-Inducible Gene *viperin* Restricts West Nile Virus Pathogenesis▽

Kristy J. Szretter,[1] James D. Brien,[1] Larissa B. Thackray,[3] Herbert W. Virgin,[2,3] Peter Cresswell,[4,5] and Michael S. Diamond[1,2,3]*

Departments of Medicine,[1] Molecular Microbiology,[2] and Pathology and Immunology,[3] Washington University School of Medicine, St. Louis, Missouri 63110, and Department of Immunobiology,[4] and Howard Hughes Medical Institute,[5] Yale University School of Medicine, New Haven, Connecticut 06520

Received 24 June 2011/Accepted 23 August 2011

Type I interferon (IFN) signaling coordinates an early antiviral program in infected and uninfected cells by inducing IFN-stimulated genes (ISGs) that modulate viral entry, replication, and assembly. However, the specific antiviral functions *in vivo* of most ISGs remain unknown. Here, we examined the contribution of the ISG viperin to the control of West Nile virus (WNV) in genetically deficient cells and mice. While modest increases in levels of WNV replication were observed for primary *viperin*$^{-/-}$ macrophages and dendritic cells, no appreciable differences were detected in deficient embryonic cortical neurons or fibroblasts. In comparison, v*iperin*$^{-/-}$ adult mice infected with WNV via the subcutaneous or intracranial route showed increased lethality and/or enhanced viral replication in central nervous system (CNS) tissues. In the CNS, viperin expression was induced in both WNV-infected and adjacent uninfected cells, including activated leukocytes at the site of infection. Our experiments suggest that viperin restricts the infection of WNV in a tissue- and cell-type-specific manner and may be an important ISG for controlling viral infections that cause CNS disease.

West Nile virus (WNV) is an enveloped, single-stranded, positive-sense RNA virus in the family *Flaviviridae*. In humans, the majority of WNV infections are asymptomatic, with a subset of individuals presenting with a febrile illness. However, in elderly or immunocompromised patients, WNV infection can progress to encephalitis and cause death (19, 38). Since 1999, more than 30,000 cases of symptomatic WNV infection have been confirmed in the United States, although seroprevalence studies suggest that this substantially underestimates the disease burden in the population (5). Currently, there is no approved therapy or vaccine for WNV in humans.

Early after cellular infection, WNV RNA is recognized by one of several nucleic acid pattern recognition receptors (RIG-I, MDA5, Toll-like receptor 3 [TLR3], and TLR7), and signaling cascades are initiated, which result in the translocation of interferon (IFN) regulatory transcription factors (IFN regulatory factor 3 [IRF-3] and IRF-7) and the induction of type I IFN (reviewed in references 11 and 62). Type I IFN binds to the IFN-α/β receptors (IFNARs) in both autocrine and paracrine fashions, activating the Janus kinase (JAK)/signal transducer and activator of transcription (STAT) pathway, which induces the expression of hundreds of interferon-stimulated genes (ISGs) (10, 30). Although several candidate inhibitory ISGs against WNV in cell culture have recently been suggested (25, 48), only 2′,5′-oligoadenylate synthetase 1b (OAS1b), double-stranded RNA protein kinase (PKR), and RNase L have confirmed antiviral activities *in vivo*. Increased susceptibility to infection by WNV and other flaviviruses expressing a nonsense mutation in the OAS1b gene has been observed in mice (33, 37), and a resistant phenotype can be attained *in vivo* after complementation with the wild-type gene (47, 55); OAS1b is an inactive oligoadenylate synthetase that restricts WNV RNA replication through an uncharacterized mechanism (15, 26, 47). Mice deficient in PKR and RNase L also showed increased lethality and viral burden after WNV infection with enhanced dissemination in neurons of the central nervous system (CNS) (46).

Viperin (*RSAD2* or *cig5*) is an ISG that is expressed in many cell types after exposure to type I and type II IFN, TLR agonists, or virus infection (7, 23, 41, 51, 64). Viperin localizes to the cytosolic face of the endoplasmic reticulum (ER) via its amphipathic α-helix (21, 22), where it is believed to contribute to antiviral effects against hepatitis C virus (HCV) (20, 24), Sindbis virus (6, 63), HIV (41), influenza virus (60), and human cytomegalovirus (HCMV) (7) by modulating cholesterol and isoprenoid biosynthesis, lipid raft formation, and the composition and localization of lipid droplets (reviewed in reference 16). The ectopic expression of viperin additionally alters ER membrane morphology, which reduces bulk protein secretion and may affect the assembly and secretion of viruses that use an ER-derived exocytic pathway (22).

As the conditional ectopic expression of viperin in fibroblasts was recently reported to reduce flavivirus infection (25), we assessed its antiviral activity *in vivo* using mice with a targeted deletion of viperin (23). *Viperin*$^{-/-}$ mice were more vulnerable to lethal WNV infection, with higher viral burdens in peripheral and central nervous system tissues. Infection experiments in deficient cells and mice suggest that viperin restricts WNV infection in a cell- and tissue-specific manner.

* Corresponding author. Mailing address: Departments of Medicine, Molecular Microbiology, and Pathology and Immunology, Washington University School of Medicine, 660 South Euclid Avenue, Campus Box 8051, St. Louis, MO 63110. Phone: (314) 362-2842. Fax: (314) 362-9230. E-mail: diamond@borcim.wustl.edu.

▽ Published ahead of print on 31 August 2011.

MATERIALS AND METHODS

Virus propagation and titration. The lineage 1 WNV strain (3000.0259) was isolated in New York in 2000 (14) and was passaged once in C6/36 *Aedes albopictus* cells to generate an insect cell-derived stock that was used in all experiments. BHK21-15 and Vero cells were used to measure viral titers of infected cells or tissues by plaque assay (12). Viremia was determined by analyzing viral RNA levels in serum using quantitative real-time reverse transcriptase PCR (qRT-PCR) and previously defined primer sets (12).

Mouse experiments and tissue preparation. C57BL/6 wild-type mice were obtained commercially (Jackson Laboratories, Bar Harbor, ME). Congenic, backcrossed *viperin*$^{-/-}$ mice were described previously (40). Eight- to 10-week-old age-matched mice were inoculated with WNV diluted in Hanks balanced salt solution (HBSS) supplemented with 1% heat-inactivated fetal bovine serum (FBS) either by footpad (10^2 PFU in 50 μl) or by intracranial (10^1 PFU in 10 μl) injection. On specific days postinfection, mice were sacrificed and perfused extensively with iced phosphate-buffered saline (PBS), and organs were harvested, weighed, and stored at −80°C until further processing. Alternatively, groups of mice were monitored for 21 days after infection for survival. All mouse experiments were performed in accordance with Washington University animal studies guidelines.

Quantification of type I IFN activity. Relative levels of biologically active type I IFN in serum were determined by using an encephalomyocarditis virus cytopathic effect bioassay with L929 cells as previously described (8). Data were expressed as international units of type I IFN per ml compared to a standard curve of recombinant IFN-α (PBL Biomedical Laboratories, NJ).

Serological analysis. WNV-specific IgM and IgG antibody levels were determined by using an enzyme-linked immunosorbent assay (ELISA) against the purified WNV E protein as previously described (34). The amount of neutralizing antibody in serum was quantitated by a focus-forming reduction assay (17).

CD8$^+$ T cell responses. Splenocytes were harvested from wild-type or *viperin*$^{-/-}$ mice on day 8 after infection. Intracellular IFN-γ or tumor necrosis factor alpha (TNF-α) staining was performed by using a D^b-restricted NS4B peptide in a restimulation assay with 1 μM peptide and 5 μg/ml of brefeldin A (Sigma) as described previously (39). Samples were processed, as described previously (57), by multicolor flow cytometry with an LSR II flow cytometer (Becton Dickinson) and analyzed with FlowJo software (Treestar).

CNS leukocyte isolation and phenotyping. The quantification of infiltrating CNS lymphocytes was based on a protocol reported previously (58). Briefly, wild-type and *viperin*$^{-/-}$ mouse brains or spinal cords were harvested on day 9 or 10 after infection, minced, and digested with a solution containing 0.05% collagenase D, 0.1 μg/ml of the trypsin inhibitor TLCK (*N*α-*p*-tosyl-L-lysine chloromethyl ketone), and 10 μg/ml DNase I in HBSS supplemented with 10 mM HEPES (pH 7.4) (Life Technologies). Cells were dispersed into single-cell suspensions with a cell strainer and centrifuged through a 37% Percoll cushion for 30 min (850 × *g* at 4°C). Cells were counted and stained either for CD3, CD4, CD8, CD45, and CD11b with directly conjugated antibodies (BD Pharmingen); for intracellular granzyme B; or for IFN-γ or TNF-α after NS4B peptide restimulation with 1 μM peptide and 5 μg/ml of brefeldin A (Sigma), as described previously (39).

Primary cell infection. Primary macrophages, dendritic cells, embryonic fibroblasts, and neurons from wild-type and *viperin*$^{-/-}$ mice were generated exactly as described previously (28, 57). Multistep virus growth curves were performed after infection at a multiplicity of infection (MOI) of 0.01. Supernatants were titrated by plaque assay on BHK21-15 cells (12). The level of WNV infection in macrophages was determined by flow cytometry. Cells were fixed with 1% paraformaldehyde, permeabilized with 0.1% saponin, and incubated with 2 μg/ml of the envelope protein-specific monoclonal antibody E16, as described previously (36). The cell viability of virus-infected cells was measured by using a Cell Titer-Glo luminescent cell viability assay (Promega) according to the manufacturer's instructions.

Immunohistochemistry and confocal microscopy. Mice were infected with 10^2 PFU of WNV via a subcutaneous route and sacrificed at day 8 after infection or with 10^1 PFU of WNV via an intracranial route and sacrificed at day 6 after infection. Following perfusion with 20 ml PBS and 20 ml 4% paraformaldehyde (PFA), brains and spinal cords were harvested and fixed in 4% PFA overnight at 4°C. Tissues were cryoprotected in 30% sucrose, and frozen sections were cut. Tissue staining was performed as previously described (57, 58). Briefly, frozen brain sections were hydrated in PBS containing 10% normal goat serum and permeabilized with 0.1% Triton X-100. Staining was performed by incubating sections overnight at 4°C with MAP2 (Chemicon), viperin (MaP.VIP [23]), or WNV (hyperimmune rat sera [12]) primary antibody. Primary antibodies were detected with secondary Alexa 488- or Alexa 555-conjugated goat anti-mouse or rat IgG (Molecular Probes). Nuclei were counterstained with ToPro-3 (Molecular Probes). Fluorescence staining was visualized and quantitated with a Zeiss 510 Meta LSM confocal microscope.

Statistical analysis. All data were analyzed by using Prism software (GraphPad Prism4). An unpaired, two-tailed *t* test was used to determine statistically significant differences for *in vitro* experiments. The Mann-Whitney test was used to analyze differences in viral burden. Kaplan-Meier survival curves were analyzed by the log rank test.

RESULTS

A deficiency of viperin results in increased susceptibility to lethal WNV infection. Viperin is an ISG that is induced to high levels after infection with a wide range of viruses and hypothesized to be a key effector molecule that restricts infection (16). Although experiments with cell cultures have suggested an antiviral effect against several RNA and DNA viruses by perturbing lipid rafts or localizing to lipid droplets (7, 24, 25, 60, 63), only one group has reported a protective effect of viperin *in vivo*, and this was in the context of ectopic expression by a viral promoter (63). To address whether an absence of viperin affects viral pathogenesis, we infected *viperin*$^{-/-}$ and wild-type mice with 10^2 PFU of WNV via a subcutaneous route (Fig. 1A). In contrast to wild-type mice, a higher percentage (62.5% versus 18.2%; $P = 0.03$) of *viperin*$^{-/-}$ mice succumbed to lethal disease. Thus, viperin has a protective effect against WNV pathogenesis *in vivo*. This result with WNV, however, was not observed when *viperin*$^{-/-}$ mice were infected with other RNA viruses corresponding to divergent families, including arenaviruses (lymphocytic choriomeningitis virus [23]) and orthomyxoviruses (influenza A virus) (data not shown). Thus, although the ectopic expression of viperin has inhibitory effects on several viruses in cell culture, its relative effect *in vivo* appears to be more limited, possibly because of redundant contributions of other inhibitory ISGs or tissue- and cell type-specific expression during infection.

Viperin restricts WNV replication in different tissues. To begin to understand how an absence of viperin causes increased mortality, we measured the WNV burden in *viperin*$^{-/-}$ and wild-type mice at different times after subcutaneous infection in serum, peripheral organs (draining lymph nodes, spleen, and kidney), and CNS tissues.

(i) Blood, lymph node, spleen, and kidney. In contrast to that observed with mice having defects in type I IFN signaling (28, 45), differences in viremia were not observed between wild-type and *viperin*$^{-/-}$ mice at days 1, 2, 3, 4, 6, and 8 after WNV infection ($P > 0.1$) (Fig. 1B). Similarly, no difference in viral replication was observed in the draining lymph node at days 1, 2, 3, 4, and 6 after WNV infection ($P < 0.1$) (Fig. 1C). However, we did detect higher viral titers in the spleen of *viperin*$^{-/-}$ mice on day 4 ($10^{5.4}$ versus $10^{4.2}$ PFU/g; $P = 0.02$) and day 5 ($10^{4.4}$ versus $10^{3.6}$ PFU/g; $P = 0.01$) after infection (Fig. 1D). We also measured higher viral titers in the kidneys of *viperin*$^{-/-}$ mice on day 4 after infection ($10^{3.1}$ versus $10^{2.0}$ PFU/g; $P = 0.03$) (Fig. 1E), an organ that is normally resistant to WNV infection but that becomes susceptible to infection in the absence of an intact type I IFN response (8, 45, 56).

(ii) Brain and spinal cord. We analyzed the effect of a viperin deficiency on the kinetics of viral replication in two CNS target tissues of WNV (54), the brain and spinal cord. Consistent with a lack of an effect on viremia, we observed no

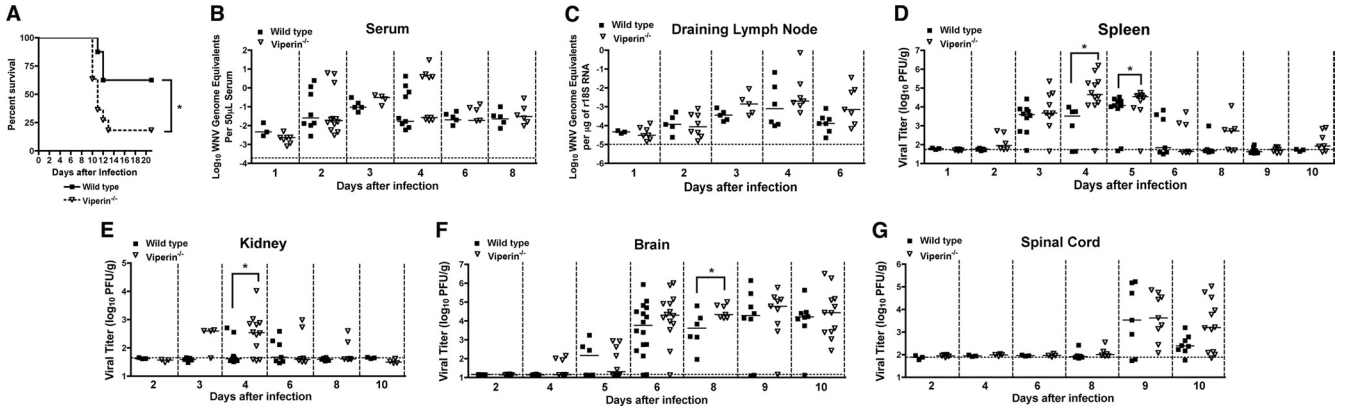

FIG. 1. Survival and viral burden analysis of wild-type and *viperin*$^{-/-}$ C57BL/6 mice. (A) Nine-week-old age-matched wild-type ($n = 8$) and *viperin*$^{-/-}$ ($n = 11$) mice were inoculated subcutaneously with 10^2 PFU of WNV, and mice were monitored for 21 days for mortality. Survival differences were statistically significant ($P = 0.03$). (B to G) WNV tissue burden and spread in mice after subcutaneous infection. *Viperin*$^{-/-}$ and wild-type mice were infected with 10^2 PFU of WNV via subcutaneous injection into the footpad. At the indicated times postinfection, tissues were harvested and analyzed for viral burden by qRT-PCR (B and C) or plaque assay (D to G). Data are shown as WNV genome equivalents per microgram of 18S rRNA (r18S) or PFU per gram of tissue for 8 to 16 mice per time point. Solid lines represent the median viral titer, and dotted lines indicate the limit of detection of the respective assays. Asterisks indicate values that are statistically significant (*, $P < 0.05$).

significant difference in the time of onset of WNV replication in the brain ($P > 0.2$ at days 4, 5, and 6). However, statistically higher viral titers were observed for *viperin*$^{-/-}$ mice on day 8 ($10^{4.6}$ versus $10^{4.2}$ PFU/g; $P = 0.04$) (Fig. 1F) after infection. While we observed an overall trend toward increased WNV replication in the spinal cord at day 10 in *viperin*$^{-/-}$ mice (Fig. 1G), this did not reach statistical significance ($P > 0.1$). However, as seen previously for adult C57BL/6 mice (4, 12), the viral burden data for the spinal cord at this time point did not fit a Gaussian distribution; while most *viperin*$^{-/-}$ mice sustained high titers, a subset were below the limit of detection ($\sim 10^2$ PFU/g) of the plaque assay. The latter data points may reflect a relatively low-level or a complete absence of CNS infection in this cohort. As the few "negative" data points create sufficient variability to limit the detection of statistical differences, we stratified the viral burden data and compared samples only from wild-type and *viperin*$^{-/-}$ mice with detectable replication in spinal cord at this time point. Using this analysis, differences in viral burden at day 10 between wild-type and *viperin*$^{-/-}$ mice became pronounced ($10^{4.4}$ versus $10^{2.6}$ PFU/g, respectively; $P = 0.0006$). Overall, an absence of viperin resulted in an increase in WNV lethality that was associated with relatively modest differences in viral replication in the CNS.

A deficiency of viperin modestly affects the IFN-α/β levels in circulation after WNV infection. A recent study showed that viperin could enhance the magnitude of TLR7- and TLR9-induced type I IFN responses by facilitating the nuclear translocation of IRF-7 in plasmacytoid dendritic cells (42). To assess whether viperin expression altered type I IFN responses *in vivo*, *viperin*$^{-/-}$ and wild-type mice were infected with WNV, and the levels of type I IFN in serum were monitored by using a previously validated L929 cell protection bioassay (1). Type I IFN activity in the serum of infected wild-type and *viperin*$^{-/-}$ mice peaked at 3 days after infection and then decreased thereafter. Notably, at 1 day after infection, we observed a small yet statistically significant decrease in the levels of type I IFN in serum in *viperin*$^{-/-}$ mice ($P < 0.05$) (Fig. 2). However, at all other time points (days 2 through 6), no difference ($P > 0.2$) in IFN-α/β levels in sera of *viperin*$^{-/-}$ mice relative to wild-type mice was observed. Thus, there appears to be a slight delay in the onset of the systemic type I IFN response after WNV infection in *viperin*$^{-/-}$ mice.

Viperin controls WNV replication in subsets of primary cells. Given the viral replication phenotype *in vivo*, we compared multistep growth kinetics in several different wild-type and *viperin*$^{-/-}$ primary cells, including macrophages and dendritic cells derived from adult mice and fibroblasts (mouse embryonic fibroblasts [MEF]) and neurons derived from mouse embryos. Notably, we observed no difference in WNV replication between wild-type and *viperin*$^{-/-}$ MEFs or neurons ($P > 0.5$) (Fig. 3A and B). In macrophages and myeloid dendritic cells, while equivalent titers were observed at 24 and 48 h postinfection, by 72 h, the level of WNV replication was sig-

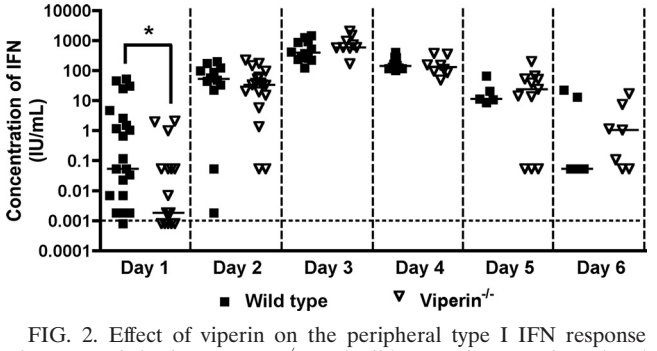

FIG. 2. Effect of viperin on the peripheral type I IFN response after WNV infection. *Viperin*$^{-/-}$ and wild-type mice were inoculated with 10^2 PFU of WNV by subcutaneous injection into the footpad. At the indicated times postinfection, serum was collected, and type I IFN activity was determined by an encephalomyocarditis virus cytopathic effect bioassay with L929 cells. The dotted line indicates the limit of detection of the assay, and data representing 5 to 15 mice at each time point are expressed as the average values on a $\log_{10}$ scale. Asterisks indicate differences that are statistically significant by the Mann-Whitney test (*, $P < 0.05$), which was performed on linear IFN levels.

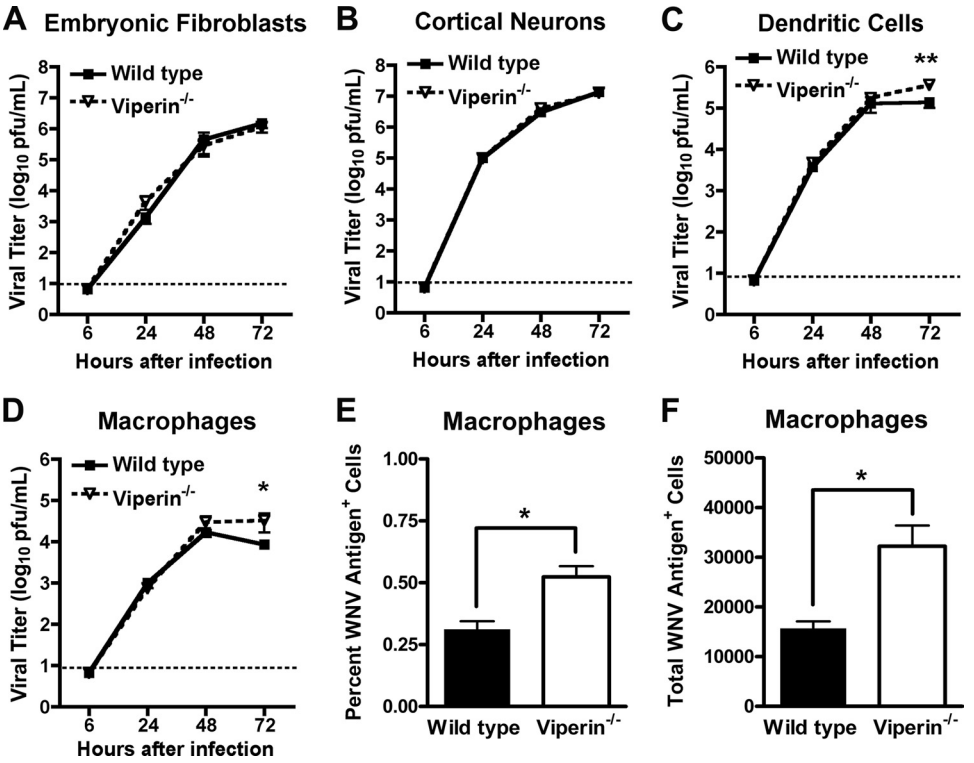

FIG. 3. Viperin restricts WNV infection in primary myeloid cells. (A to D) Fibroblasts (A) and cortical neurons (B) were generated from embryos of wild-type and *viperin*$^{-/-}$ mice, and bone marrow-derived dendritic cells (C) and macrophages (D) were isolated from adult wild-type and *viperin*$^{-/-}$ mice. Primary cells were infected at an MOI of 0.01, and the virus yield was titrated at the indicated times by plaque assay on BHK21-15 or Vero cells. Values are averages of values from triplicate samples generated from at least three independent experiments. The dotted line represents the limit of detection for the assay. (E and F) WNV-infected macrophages were harvested 72 h after infection, stained with WNV-specific monoclonal antibody E16, and analyzed by flow cytometry. Asterisks indicate values that are statistically different (*, $P < 0.05$; **, $P < 0.005$).

nificantly higher in *viperin*$^{-/-}$ myeloid cells ($P < 0.02$) (Fig. 3C and D). To corroborate these findings, we harvested WNV-infected macrophages 72 h after infection, stained cells for viral antigen, and analyzed cells by flow cytometry. We observed a significant increase in both the percentage and number of WNV-infected *viperin*$^{-/-}$ macrophages compared to those of wild-type cells ($P < 0.02$) (Fig. 3E and F). To determine whether the increase in virus yield in *viperin*$^{-/-}$ myeloid cells was related to enhanced cell survival, we measured cell viability by quantifying levels of intracellular ATP as an indicator of metabolic activity. While we observed an 8.4% increase ($P = 0.04$) in relative viability in *viperin*$^{-/-}$ macrophages at 72 h, no difference ($P > 0.5$) was observed for dendritic cells (data not shown). Overall, our results establish a cell type-specific effect of viperin on WNV replication, with little impact on replication in primary neurons and fibroblasts. This absence of an effect was not due to a lack of cell type-specific induction, as cortical neurons showed a 4,000-fold increase in viperin mRNA levels within 24 h after WNV infection, levels that were similar to those observed in macrophages (data not shown).

Effect of viperin on T and B cell responses to WNV infection. Although *viperin*$^{-/-}$ mice show normal hematopoietic cell development, *viperin*$^{-/-}$ CD4$^+$ T cells produced smaller amounts of Th2 cytokines (interleukin-4 [IL-4], IL-5, and IL-13) and IgG1 antibodies after immunization with ovalbumin (40). Viperin is also highly expressed in antigen-presenting cells during viral infection (23) and could influence T cell priming by virtue of its ability to promote type I IFN production in plasmacytoid dendritic cells (42). As depressed antiviral CD8$^+$ T cell and antibody responses can facilitate enhanced dissemination and replication of WNV *in vivo* (3, 12, 53, 61), we investigated whether an absence of viperin influenced the development of an effective adaptive immune response during infection.

At day 8 after WNV infection, splenocytes were harvested from wild-type and *viperin*$^{-/-}$ mice and restimulated *ex vivo* with a D^b-restricted immunodominant WNV NS4B peptide (3, 39). Equivalent percentages and numbers of total CD8$^+$ T cells were isolated from wild-type and *viperin*$^{-/-}$ mice ($P > 0.2$) (Fig. 4B and data not shown). Notably, we observed no difference in the percentages or numbers of WNV-specific CD8$^+$ T cells expressing IFN-γ, TNF-α, or granzyme B ($P > 0.2$) (Fig. 4A, C, and D and data not shown) in wild-type and *viperin*$^{-/-}$ mice.

Although peripheral antigen-specific CD8$^+$ T cell responses against WNV developed normally in *viperin*$^{-/-}$ mice, we assessed whether leukocyte migration to the CNS might be altered, which could impact viral clearance (18, 27, 59). Leukocytes were isolated from brains of wild-type and *viperin*$^{-/-}$ mice at day 9 and from spinal cords at day 10 after extensive perfusion and analyzed by flow cytometry. In the brain, we observed similar accumulations of total CD3$^+$ CD4$^+$ and

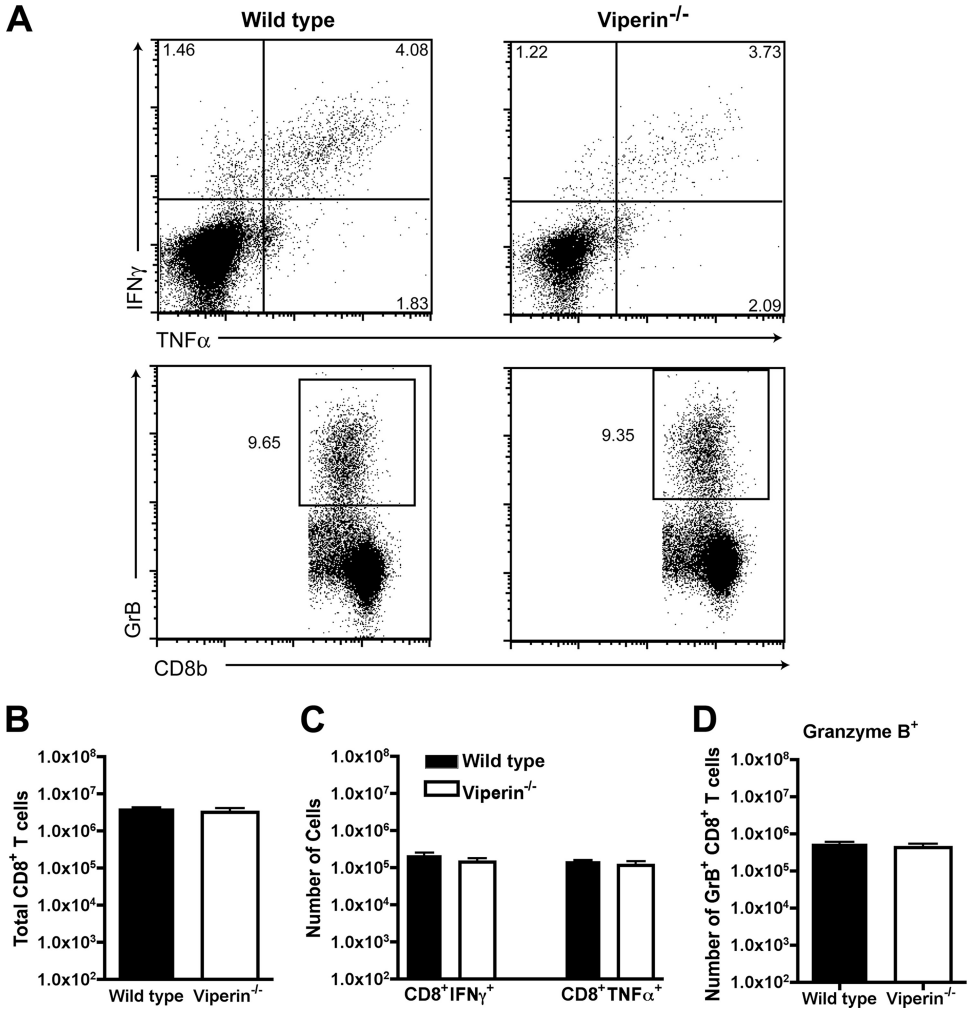

FIG. 4. Peripheral T cell responses after WNV infection in *viperin*$^{-/-}$ mice. Wild-type and *viperin*$^{-/-}$ mice were inoculated with 10^2 PFU of WNV by footpad injection, and spleens were harvested on day 8. (A, top) Flow cytometry dot plots showing intracellular IFN-γ and TNF-α cells after gating on CD8α$^+$ T cells. Cells were restimulated *ex vivo* with a D^b-restricted NS4b peptide. (Bottom) Intracellular expression of granzyme B (GrB) in CD8$^+$ T cells from WNV-infected mice. (B) Bulk numbers of splenic CD8$^+$ T cells at day 8 after infection in wild-type and *viperin*$^{-/-}$ mice. (C and D) Leukocytes were stained for granzyme B expression or stimulated with the NS4b peptide, incubated with antibodies for CD3 and CD8 and IFN-γ or TNF-α, and analyzed by flow cytometry. Data are shown as the total numbers of CD3$^+$ CD8$^+$ T cells that expressed intracellular granzyme B, IFN-γ, or TNF-α after peptide restimulation. The differences were not statistically significant, and the data were pooled from three independent experiments with a total of 7 to 8 mice.

CD3$^+$ CD8$^+$ T cells ($P > 0.1$) (Fig. 5A) and WNV-specific CD8$^+$ T cells expressing IFN-γ or TNF-α ($P > 0.3$) (Fig. 5B) or granzyme B ($P > 0.8$) (Fig. 5C). We also did not observe any difference in the accumulations of activated microglia (CD11b^{high} CD45^{low}) or macrophages (CD11b^{high} CD45^{high}) ($P > 0.4$) (Fig. 5D). For the spinal cord, we had similar results ($P > 0.1$) (Fig. 5E to G), with the exception of a trend toward slightly higher numbers of T cells expressing granzyme B ($P = 0.08$) (Fig. 5E) in *viperin*$^{-/-}$ mice, although this did not attain statistical significance. In comparison, no statistical difference in the numbers of activated microglia and macrophages was observed for the spinal cord of WNV-infected mice at day 10 ($P > 0.3$) (Fig. 5H). These data suggest that a deficiency of viperin does not adversely affect the recruitment of antigen-specific and nonspecific immune cells in the CNS of WNV-infected mice.

To assess the effect of viperin on WNV-specific antibody responses, we analyzed serum from *viperin*$^{-/-}$ and wild-type mice on days 6, 8, and 10 after infection for binding to the WNV E protein. At days 6 and 8, no differences were observed. However, at day 10, *viperin*$^{-/-}$ mice had higher levels of WNV-specific IgM (geometric mean titers of 1/770 and 1/270; $P < 0.05$) (Fig. 6A) and IgG (geometric mean titers of 1/8,230 and 1/2,330; $P = 0.01$) (Fig. 6B) in serum. To evaluate whether the anti-WNV antibody from *viperin*$^{-/-}$ mice was functionally relevant, we performed a focus reduction neutralization test. Notably, no statistical difference in the neutralizing activities of serum was detected in sera from *viperin*$^{-/-}$ and wild-type mice at day 6, 8, or 10 ($P > 0.3$) (Fig. 6C). The slight disparity between increased absolute antibody titers and no difference in neutralizing activity suggests a qualitative change in the anti-WNV antibody response in *viperin*$^{-/-}$ mice; a similar pattern

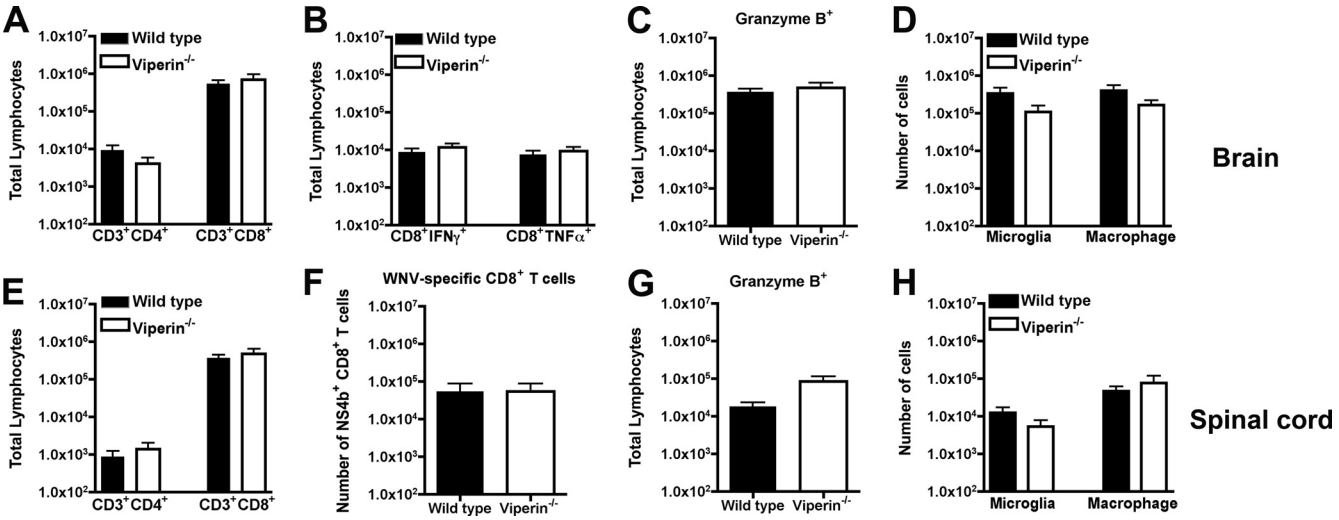

FIG. 5. Leukocyte accumulation in the CNS of *viperin*$^{-/-}$ mice after WNV infection. Wild-type and *viperin*$^{-/-}$ mice were inoculated with 10^2 PFU of WNV by subcutaneous injection into the footpad. Brains (A to D) and spinal cords (E to H) were harvested on days 9 and 10, respectively, and leukocytes were isolated by Percoll gradient centrifugation. (A and E) The total number of $CD3^+$ $CD4^+$ or $CD3^+$ $CD8^+$ T cells was determined by multiplying the percentage of $CD3^+$ $CD8^+$ cells by the total cell count. (B and C) Brain leukocytes were stimulated *ex vivo* with a D^b-restricted NS4b WNV peptide; stained for CD3 and CD8 and intracellular granzyme B, IFN-γ, or TNF-α; and analyzed by flow cytometry. (F and G) Spinal cord leukocytes were stained directly with D^b-NS4b tetramers and antibodies to CD8 and granzyme B. (D and H) The numbers of macrophages ($CD11b^{high}/CD45^{high}$) and microglia ($CD11b^{high}/CD45^{low}$) were also measured. Differences were not statistically significant, and data represent the averages of data from 3 to 4 independent experiments with 3 to 5 mice per experiment (n = 11 to 19).

was also observed previously for WNV-infected *IPS-1*$^{-/-}$ mice (56). Nonetheless, the virological phenotype observed for *viperin*$^{-/-}$ mice did not appear to be due to major defects in T or B cell function.

Viperin has a role in restricting WNV replication in the CNS. Because previous studies showed direct antiviral effects of type I IFN and ISGs on the CNS (45, 46, 57), we hypothesized that viperin could restrict WNV replication in the brain through inhibitory effects on neuronal infection. To test this, wild-type and *viperin*$^{-/-}$ mice were infected with 10^1 PFU of WNV directly in the cerebral cortex via an intracranial route, and viral burdens in the cerebral cortex, white matter, brain stem, cerebellum, and spinal cord were measured on days 2, 4, and 6 after infection. At day 2 after infection, no difference in WNV infection was detected for any of the CNS tissues between wild-type and *viperin*$^{-/-}$ mice. However, by day 4, higher titers were measured in the cortex ($10^{7.9}$ versus $10^{6.8}$ PFU/g; $P = 0.02$), white matter ($10^{7.6}$ versus $10^{6.4}$ PFU/g; $P = 0.02$), and spinal cord ($10^{4.1}$ versus $10^{2.9}$ PFU/g; $P = 0.004$) of *viperin*$^{-/-}$ mice than of wild-type mice. The enhanced replication in *viperin*$^{-/-}$ mice was sustained at day 6 in the cortex ($10^{8.8}$ versus $10^{8.1}$ PFU/g; $P = 0.04$) and spinal cord ($10^{5.8}$ versus $10^{4.8}$ PFU/g; $P = 0.023$) (Fig. 7A, B, and E). However, the differences in CNS replication in *viperin*$^{-/-}$ mice were regional, as an equivalent infection was observed for the brain stem ($P > 0.9$) (Fig. 7C) and cerebellum ($P > 0.4$) (Fig. 7D) at all time points. These data suggest that the antiviral function of viperin may be important in restricting spread to and infection of subsets of neuronal cells in the CNS.

Viperin is differentially expressed at sites of WNV infection in the CNS in infected and uninfected cells. Given that its absence resulted in enhanced WNV infection in specific regions of the brain, we hypothesized that viperin might preferentially restrict infection in specific CNS cell types. To assess this, immunohistochemical and confocal microscopy analyses were performed on CNS tissues at day 6 after intracranial infection. In the brain and spinal cord, WNV infection occurred predominantly in neurons, with higher numbers of infected neurons apparent in *viperin*$^{-/-}$ mice (data not shown). While viperin staining was appreciated readily for the cortex (Fig. 8A), hippocampus (Fig. 8B), cerebellum (Fig. 8C), and brain stem (Fig. 8D), it was present in both WNV-infected (Fig. 8, arrows) and uninfected (arrowheads) cells in these regions, possibly due to local paracrine effects of type I IFN secretion from virus-infected neurons (8, 9) or trafficking leukocytes that were stimulated by IFN in the periphery (23). In contrast, staining in the spinal cord showed a distinct pattern: viperin antigen colocalized only with WNV-infected cells in the gray matter regions (Fig. 8E to G, arrows). Similar viperin staining patterns in the brain and spinal cord were observed at day 10 after subcutaneous infection with WNV (data not shown). Importantly, as controls, viperin staining was not observed for WNV-infected brain or spinal cord sections from *viperin*$^{-/-}$ mice (Fig. 8H and I) or mock-infected sections from wild-type mice (Fig. 8J). Thus, while viperin was coexpressed in infected cells throughout the CNS, in uninfected cells, it appeared to be differentially induced in a region-specific manner.

DISCUSSION

Whereas previous studies had identified viperin as a candidate antiviral ISG in cell cultures using either ectopic expression or RNA interference approaches, we establish its role in restricting the pathogenesis of viral infection in mice.

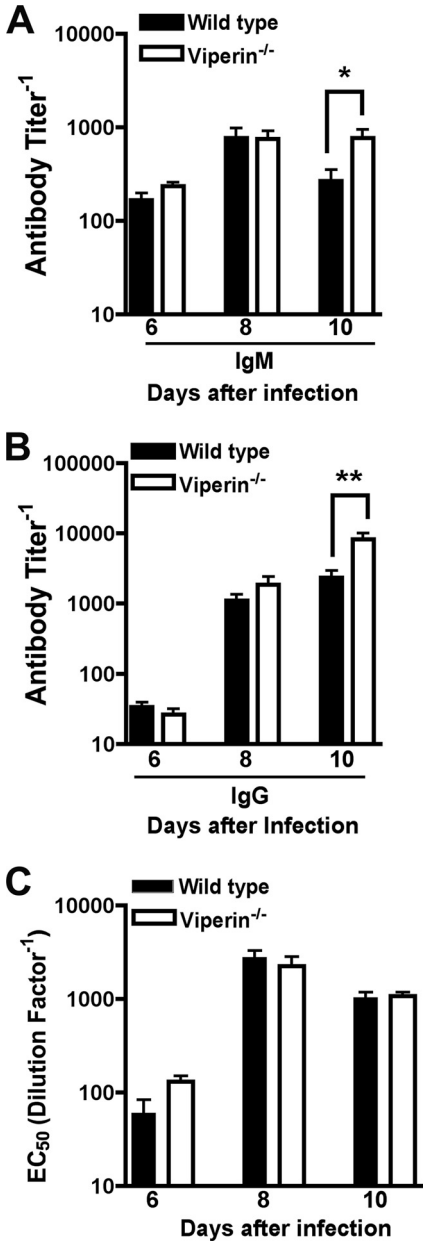

FIG. 6. WNV-specific antibody responses in *viperin*$^{-/-}$ mice. Wild-type and *viperin*$^{-/-}$ mice were infected with 10^2 PFU of WNV by subcutaneous injection into the footpad. At the indicated times postinfection, serum was collected and assayed by ELISA for WNV E-specific IgM (A) and IgG (B) antibody titers. Data represent the reciprocal endpoint titers. (C) Sera from the indicated times postinfection were tested for neutralization activity using a focus reduction assay. Data represent the effective concentration that produced 50% neutralization of WNV infection (EC_{50}). Asterisks indicate values that are statistically significant (*, $P < 0.05$; **, $P < 0.005$).

Viperin$^{-/-}$ mice showed enhanced susceptibility to lethal WNV infection, and this was associated with elevated levels of replication in subsets of peripheral and CNS tissues. A direct effect of viperin on neuronal infection and spread *in vivo* was also suggested, as deficient mice exhibited higher viral burdens in CNS tissues following direct intracranial inoculation. This finding was associated with regional effects on viperin expression after viral infection in different parts of the brain and spinal cord but not with marked differences in neuronal death (data not shown). Finally, a multistep viral growth analysis of primary cells corroborated a cell type-specific antiviral function of viperin, as *viperin*$^{-/-}$ myeloid cells but not embryonic fibroblasts or cortical neurons showed enhanced infectivity.

Cell culture experiments have suggested that viperin, an ER-associated protein that is strongly induced by type I IFN signaling, has antiviral activity against an array of RNA and DNA viruses. Initial experiments showed that the stable ectopic expression of viperin inhibited HCMV assembly and maturation (7). Subsequent studies showed that the expression of viperin decreased the replication of HCV (20, 24), Sindbis virus (6, 63), and influenza viruses (60). Analogously, small interfering RNA (siRNA) knockdown of viperin reversed the poly(I · C)-induced inhibition of HIV replication (41). Despite the cell culture data suggesting that viperin was an antiviral ISG against several viruses, there has been little evidence for its function *in vivo*. Prior to our study with WNV and *viperin*$^{-/-}$ mice, only one report suggested an antiviral role for viperin *in vivo*: the ectopic expression of viperin in a recombinant Sindbis virus enhanced protection against lethal infection in neonatal CD1 mice (63). In comparison, no statistically significant difference in viral burden was observed for *viperin*$^{-/-}$ mice compared to wild-type mice after infection with lymphocytic choriomeningitis virus (23). One explanation as to why major gain-of-function phenotypes are not consistently observed in *viperin*$^{-/-}$ mice is that multiple ISGs function in concert to inhibit viral replication *in vivo*. Alternatively, a cell type- or tissue-specific expression pattern of viperin could contribute to the limited viral burden or lethality phenotypes in infection models with *viperin*$^{-/-}$ mice that have been studied to date. Finally, as another possibility, and as was shown recently, some viruses (e.g., HCMV) may directly co-opt the enzymatic activity of viperin to enhance infectivity (50).

Our experiments show that an absence of viperin results in enhanced WNV infectivity in cell culture and *in vivo*, results that both support and conflict with previous studies with flaviviruses. The ectopic expression of viperin in HEK-293 cells inhibited the replication of dengue virus (DENV) and WNV (25). The deletion of the N-terminal α-helical region of viperin, which is required for its association with the ER membrane, did not completely abolish its antiviral activity. However, the expression of a mutant viperin with substitutions of essential cysteines in a motif required for radical *S*-adenosyl methionine enzymatic activity (13, 24, 52) had virtually no antiviral activity against WNV and DENV (25). Nonetheless, other large-scale genetic screens of the antiviral activity of ISG using lentivirus-based ectopic expression platforms did not identify viperin as an antiviral gene for WNV or yellow fever virus (48). Some flaviviruses may actively antagonize viperin activity by targeting it for degradation. While viperin is highly induced at the mRNA level in Japanese encephalitis virus-infected cells, the protein is rapidly degraded through a proteasome-dependent mechanism in human A549 cells (6). Given our data showing cell type-, tissue-, and region-specific effects and the expres-

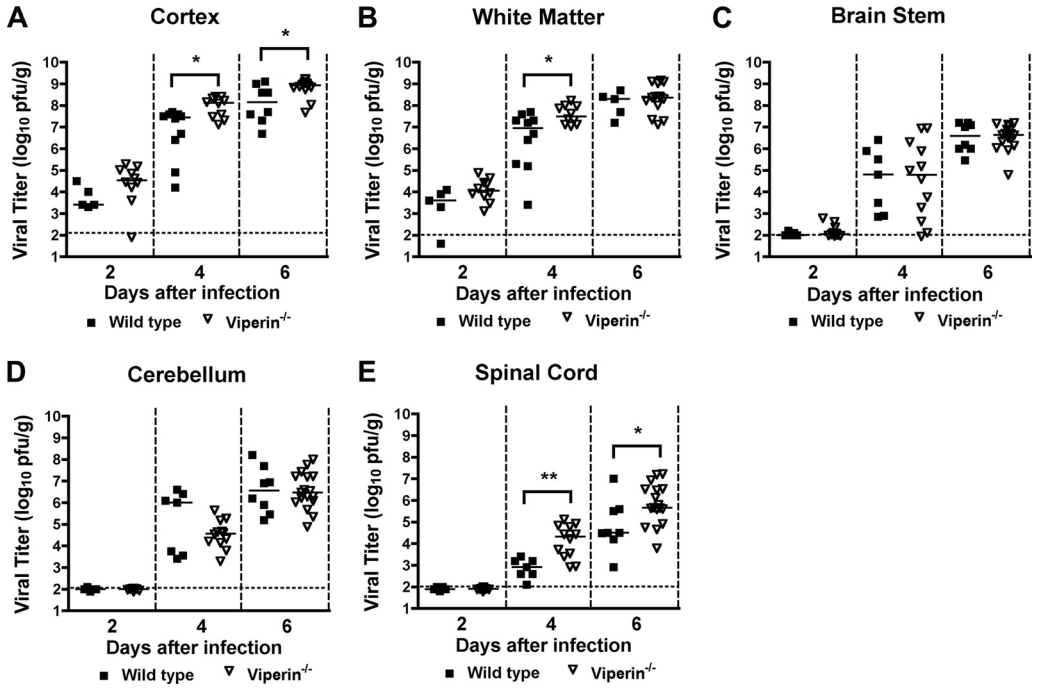

FIG. 7. WNV replication in regions of the CNS of *viperin*$^{-/-}$ mice after intracranial infection. *Viperin*$^{-/-}$ and wild-type mice were infected with 10^1 PFU WNV via intracranial injection. At the indicated times postinfection, cerebral cortex (gray matter) (A), white matter (B), brain stem (C), cerebellum (D), and spinal cord (E) were harvested and analyzed for viral burden by plaque assay on BHK21-15 cells. Data are shown as PFU per gram of tissue for 7 to 17 mice per time point. Solid lines represent the median viral titers, and dotted lines indicate the limit of detection of the respective assays. Asterisks indicate values that are statistically significant (*, $P < 0.05$; **, $P < 0.005$).

sion of viperin in the context of WNV infection, the variation observed by investigators may be due to context-dependent cellular requirements for viperin. For studies that knock down or delete the expression of viperin, a redundancy of function of other ISGs could compensate such that the loss of viperin has minimal effects. Correspondingly, ectopic expression may not be sufficient for antiviral effects in specific cell types due to requirements for activation or association with other antiviral proteins.

How does viperin inhibit WNV infection? Viperin has been proposed to have antiviral functions through multiple mechanisms (reviewed in reference 16). Viperin contains an N-terminal amphipathic α-helix that localizes to the cytosolic face of the ER and inhibits bulk protein secretion (22), which could impact virus production directly or indirectly. Indeed, our experiments with macrophages but not dendritic cells suggest that viperin induction may affect WNV replication indirectly, by modulating cell survival. Viperin also inhibits farnesyl diphosphate synthetase, a cholesterol and isoprenoid biosynthesis enzyme, resulting in the inhibition of lipid raft formation and influenza virus budding (60). However, flaviviruses and HCV virions do not bud from lipid rafts but instead assemble in the ER of infected cells and are secreted through cellular exocytic pathways (29). As it localizes to ER-derived lipid droplets, which are required for efficient HCV and flavivirus replication (2, 35, 43), viperin could alter viral protein localization or the precise lipid content. Alternatively, viperin could enhance the magnitude of TLR7- and TLR9-induced type I IFN responses by facilitating the nuclear translocation of IRF-7, as described previously for plasmacytoid dendritic cells (42). We observed only a small delay in the type I IFN systemic response in *viperin*$^{-/-}$ mice within the first 24 h of WNV infection.

The identification of viperin as an ISG that restricts WNV infection *in vivo* adds to a remarkably small amount of literature showing that the deletion of individual ISGs can impact pathogenesis. The redundancy of the antiviral IFN system likely results in relatively modest phenotypes when individual ISGs are deleted compared to the targeted knockout of the type I IFN receptor, pathogen recognition receptors, or key IRF signaling intermediates (11, 44), which initiate the induction of hundreds of ISGs. Previous experiments in mice showed that the deletion of PKR, RNase L, or OAS1b correlated with increased susceptibility to WNV in mice (33, 37, 46), although more recent works suggested that at least some of the phenotypes (for PKR and RNase L) could be due to amplification rather than an execution of IFN signals (31, 32, 49). Given the increasing number of putative antiviral ISGs that regulate infection by WNV and other viruses (48), the expectation that the targeted deletion of any single gene will have dramatic effects may be unrealistic, and the more modest phenotype observed with *viperin*$^{-/-}$ mice should be expected.

In summary, our results show that viperin contributes to the antiviral responses against WNV *in vivo*, as the targeted deletion of viperin was associated with increased lethality and selectively enhanced replication in specific tissues, without an appreciable effect of the innate or adaptive CD8$^+$ T cell or antibody responses. Based on tissue-specific and regional effects and replication studies with primary cells, we postulate a model in which distinct cell types differentially utilize viperin to

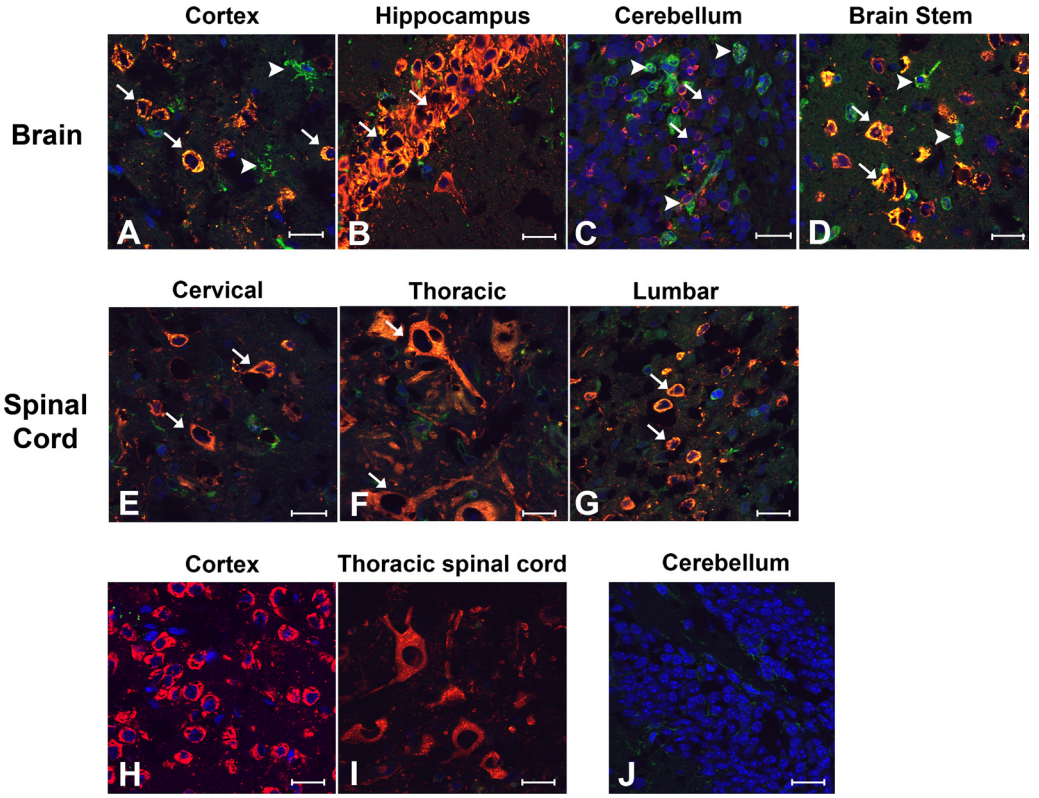

FIG. 8. Viperin protein expression in the CNS after WNV infection. Wild-type mice were infected with 10^1 PFU WNV via intracranial injection. At day 6, tissues were harvested and processed as described in Materials and Methods. (A to G) Fixed, frozen sections from the cerebral cortex (A); hippocampus (B); cerebellum (C); brain stem (D); and cervical (E), thoracic (F), and lumbar (G) spinal cord were costained for WNV antigen (red), viperin (green), and the nuclear stain ToPro-3 (blue). Images are representative of 4 to 6 wild-type mice. Arrows define cells that were WNV infected and stained positive for viperin, whereas arrowheads denote cells that stained positive for viperin but were not appreciably infected. (H to J) Representative images from WNV-infected *viperin*$^{-/-}$ cerebral cortex (H) and thoracic spinal cord (I) and mock-infected wild-type cerebellum (J) were also included as staining controls. Bars indicate a 20-μm scale.

inhibit WNV infection. As cell-specific antiviral programs induced by type I IFN may differ in both the kinetics and repertoires of IFN-induced antiviral proteins, a more detailed pathogenesis analysis may reveal when and how viperin restricts the infection of specific RNA and DNA viruses.

ACKNOWLEDGMENTS

NIH grants U54 AI081680 and U54 AI057160 (Pacific Northwest and Midwest Regional Centers of Excellence for Biodefense and Emerging Infectious Diseases Research) and U19 AI083019 supported this work. K.J.S. was supported an NIH training grant, T32-AI007172.

REFERENCES

1. **Austin, B. A., C. James, R. H. Silverman, and D. J. Carr.** 2005. Critical role for the oligoadenylate synthetase/RNase L pathway in response to IFN-beta during acute ocular herpes simplex virus type 1 infection. J. Immunol. **175:** 1100–1106.
2. **Boulant, S., P. Targett-Adams, and J. McLauchlan.** 2007. Disrupting the association of hepatitis C virus core protein with lipid droplets correlates with a loss in production of infectious virus. J. Gen. Virol. **88:**2204–2213.
3. **Brien, J. D., J. L. Uhrlaub, and J. Nikolich-Zugich.** 2007. Protective capacity and epitope specificity of CD8(+) T cells responding to lethal West Nile virus infection. Eur. J. Immunol. **37:**1855–1863.
4. **Brown, A. N., K. A. Kent, C. J. Bennett, and K. A. Bernard.** 2007. Tissue tropism and neuroinvasion of West Nile virus do not differ for two mouse strains with different survival rates. Virology **368:**422–430.
5. **Busch, M. P., et al.** 2006. West Nile virus infections projected from blood donor screening data, United States, 2003. Emerg. Infect. Dis. **12:**395–402.
6. **Chan, Y. L., T. H. Chang, C. L. Liao, and Y. L. Lin.** 2008. The cellular antiviral protein viperin is attenuated by proteasome-mediated protein degradation in Japanese encephalitis virus-infected cells. J. Virol. **82:**10455–10464.
7. **Chin, K. C., and P. Cresswell.** 2001. Viperin (cig5), an IFN-inducible antiviral protein directly induced by human cytomegalovirus. Proc. Natl. Acad. Sci. U. S. A. **98:**15125–15130.
8. **Daffis, S., M. A. Samuel, B. C. Keller, M. Gale, Jr., and M. S. Diamond.** 2007. Cell-specific IRF-3 responses protect against West Nile virus infection by interferon-dependent and independent mechanisms. PLoS Pathog. **3:**e106.
9. **Delhaye, S., et al.** 2006. Neurons produce type I interferon during viral encephalitis. Proc. Natl. Acad. Sci. U. S. A. **103:**7835–7840.
10. **Der, S. D., A. Zhou, B. R. Williams, and R. H. Silverman.** 1998. Identification of genes differentially regulated by interferon alpha, beta, or gamma using oligonucleotide arrays. Proc. Natl. Acad. Sci. U. S. A. **95:**15623–15628.
11. **Diamond, M. S.** 2009. Mechanisms of evasion of the type I interferon antiviral response by flaviviruses. J. Interferon Cytokine Res. **29:**521–530.
12. **Diamond, M. S., B. Shrestha, A. Marri, D. Mahan, and M. Engle.** 2003. B cells and antibody play critical roles in the immediate defense of disseminated infection by West Nile encephalitis virus. J. Virol. **77:**2578–2586.
13. **Duschene, K. S., and J. B. Broderick.** 2010. The antiviral protein viperin is a radical SAM enzyme. FEBS Lett. **584:**1263–1267.
14. **Ebel, G. D., J. Carricaburu, D. Young, K. A. Bernard, and L. D. Kramer.** 2004. Genetic and phenotypic variation of West Nile virus in New York, 2002–2003. Am. J. Trop. Med. Hyg. **71:**493–500.
15. **Elbahesh, H., B. K. Jha, R. H. Silverman, S. V. Scherbik, and M. A. Brinton.** 2011. The Flvr-encoded murine oligoadenylate synthetase 1b (Oas1b) suppresses 2-5A synthesis in intact cells. Virology **409:**262–270.
16. **Fitzgerald, K. A.** 2011. The interferon inducible gene: viperin. J. Interferon Cytokine Res. **31:**131–135.
17. **Fuchs, A., A. K. Pinto, W. J. Schwaeble, and M. S. Diamond.** 2011. The lectin pathway of complement activation contributes to protection from West Nile virus infection. Virology **412:**101–109.
18. **Glass, W. G., et al.** 2005. Chemokine receptor CCR5 promotes leukocyte

trafficking to the brain and survival in West Nile virus infection. J. Exp. Med. **202:**1087–1098.
19. **Hayes, E. B., et al.** 2005. Epidemiology and transmission dynamics of West Nile virus disease. Emerg. Infect. Dis. **11:**1167–1173.
20. **Helbig, K. J., D. T. Lau, L. Semendric, H. A. Harley, and M. R. Beard.** 2005. Analysis of ISG expression in chronic hepatitis C identifies viperin as a potential antiviral effector. Hepatology **42:**702–710.
21. **Hinson, E. R., and P. Cresswell.** 2009. The antiviral protein, viperin, localizes to lipid droplets via its N-terminal amphipathic alpha-helix. Proc. Natl. Acad. Sci. U. S. A. **106:**20452–20457.
22. **Hinson, E. R., and P. Cresswell.** 2009. The N-terminal amphipathic alpha-helix of viperin mediates localization to the cytosolic face of the endoplasmic reticulum and inhibits protein secretion. J. Biol. Chem. **284:**4705–4712.
23. **Hinson, E. R., et al.** 2010. Viperin is highly induced in neutrophils and macrophages during acute and chronic lymphocytic choriomeningitis virus infection. J. Immunol. **184:**5723–5731.
24. **Jiang, D., et al.** 2008. Identification of three interferon-inducible cellular enzymes that inhibit the replication of hepatitis C virus. J. Virol. **82:**1665–1678.
25. **Jiang, D., et al.** 2010. Identification of five interferon-induced cellular proteins that inhibit West Nile virus and dengue virus infections. J. Virol. **84:**8332–8341.
26. **Kajaste-Rudnitski, A., et al.** 2006. The 2′,5′-oligoadenylate synthetase 1b is a potent inhibitor of West Nile virus replication inside infected cells. J. Biol. Chem. **281:**4624–4637.
27. **Klein, R. S., et al.** 2005. Neuronal CXCL10 directs CD8+ T cell recruitment and control of West Nile virus encephalitis. J. Virol. **79:**11457–11466.
28. **Lazear, H. M., A. K. Pinto, M. R. Vogt, M. Gale, Jr., and M. S. Diamond.** 2011. Beta interferon controls West Nile virus infection and pathogenesis in mice. J. Virol. **85:**7186–7194.
29. **Lindenbach, B. D., and C. M. Rice.** 2001. Flaviviridae: the viruses and their replication, p. 991–1041. *In* D. M. Knipe et al. (ed.), Fields virology, 4th ed., vol. 1. Lippincott Williams & Wilkins, Philadelphia, PA.
30. **Liu, S. Y., D. J. Sanchez, and G. Cheng.** 2011. New developments in the induction and antiviral effectors of type I interferon. Curr. Opin. Immunol. **23:**57–64.
31. **Malathi, K., B. Dong, M. Gale, Jr., and R. H. Silverman.** 2007. Small self-RNA generated by RNase L amplifies antiviral innate immunity. Nature **448:**816–819.
32. **Malathi, K., et al.** 2010. RNase L releases a small RNA from HCV RNA that refolds into a potent PAMP. RNA **16:**2108–2119.
33. **Mashimo, T., et al.** 2002. A nonsense mutation in the gene encoding 2′-5′-oligoadenylate synthetase/L1 isoform is associated with West Nile virus susceptibility in laboratory mice. Proc. Natl. Acad. Sci. U. S. A. **99:**11311–11316.
34. **Mehlhop, E., and M. S. Diamond.** 2006. Protective immune responses against West Nile virus are primed by distinct complement activation pathways. J. Exp. Med. **203:**1371–1381.
35. **Miyanari, Y., et al.** 2007. The lipid droplet is an important organelle for hepatitis C virus production. Nat. Cell Biol. **9:**1089–1097.
36. **Oliphant, T., et al.** 2005. Development of a humanized monoclonal antibody with therapeutic potential against West Nile virus. Nat. Med. **11:**522–530.
37. **Perelygin, A. A., et al.** 2002. Positional cloning of the murine flavivirus resistance gene. Proc. Natl. Acad. Sci. U. S. A. **99:**9322–9327.
38. **Petersen, L. R., A. A. Marfin, and D. J. Gubler.** 2003. West Nile virus. JAMA **290:**524–528.
39. **Purtha, W. E., et al.** 2007. Antigen-specific cytotoxic T lymphocytes protect against lethal West Nile virus encephalitis. Eur. J. Immunol. **37:**1845–1854.
40. **Qiu, L. Q., P. Cresswell, and K. C. Chin.** 2009. Viperin is required for optimal Th2 responses and T-cell receptor-mediated activation of NF-kappaB and AP-1. Blood **113:**3520–3529.
41. **Rivieccio, M. A., et al.** 2006. TLR3 ligation activates an antiviral response in human fetal astrocytes: a role for viperin/cig5. J. Immunol. **177:**4735–4741.
42. **Saitoh, T., et al.** 2011. Antiviral protein viperin promotes Toll-like receptor 7- and Toll-like receptor 9-mediated type I interferon production in plasmacytoid dendritic cells. Immunity **34:**352–363.
43. **Samsa, M. M., et al.** 2009. Dengue virus capsid protein usurps lipid droplets for viral particle formation. PLoS Pathog. **5:**e1000632.
44. **Samuel, M. A., and M. S. Diamond.** 2006. Pathogenesis of West Nile virus infection: a balance between virulence, innate and adaptive immunity, and viral evasion. J. Virol. **80:**9349–9360.
45. **Samuel, M. A., and M. S. Diamond.** 2005. Alpha/beta interferon protects against lethal West Nile virus infection by restricting cellular tropism and enhancing neuronal survival. J. Virol. **79:**13350–13361.
46. **Samuel, M. A., et al.** 2006. PKR and RNase L contribute to protection against lethal West Nile virus infection by controlling early viral spread in the periphery and replication in neurons. J. Virol. **80:**7009–7019.
47. **Scherbik, S. V., K. Kluetzman, A. A. Perelygin, and M. A. Brinton.** 2007. Knock-in of the Oas1b (r) allele into a flavivirus-induced disease susceptible mouse generates the resistant phenotype. Virology **368:**232–237.
48. **Schoggins, J. W., et al.** 2011. A diverse range of gene products are effectors of the type I interferon antiviral response. Nature **472:**481–485.
49. **Schulz, O., et al.** 2010. Protein kinase R contributes to immunity against specific viruses by regulating interferon mRNA integrity. Cell Host Microbe **7:**354–361.
50. **Seo, J. Y., R. Yaneva, E. R. Hinson, and P. Cresswell.** 2011. Human cytomegalovirus directly induces the antiviral protein viperin to enhance infectivity. Science **332:**1093–1097.
51. **Severa, M., E. M. Coccia, and K. A. Fitzgerald.** 2006. Toll-like receptor-dependent and -independent viperin gene expression and counter-regulation by PRDI-binding factor-1/BLIMP1. J. Biol. Chem. **281:**26188–26195.
52. **Shaveta, G., J. Shi, V. T. Chow, and J. Song.** 2010. Structural characterization reveals that viperin is a radical S-adenosyl-L-methionine (SAM) enzyme. Biochem. Biophys. Res. Commun. **391:**1390–1395.
53. **Shrestha, B., and M. S. Diamond.** 2004. The role of CD8+ T cells in the control of West Nile virus infection. J. Virol. **78:**8312–8321.
54. **Shrestha, B., D. I. Gottlieb, and M. S. Diamond.** 2003. Infection and injury of neurons by West Nile encephalitis virus. J. Virol. **77:**13203–13213.
55. **Simon-Chazottes, D., et al.** 2011. Transgenic expression of full-length 2′,5′-oligoadenylate synthetase 1b confers to BALB/c mice resistance against West Nile virus-induced encephalitis. Virology **417:**147–153.
56. **Suthar, M. S., et al.** 2010. IPS-1 is essential for the control of West Nile virus infection and immunity. PLoS Pathog. **6:**e1000757.
57. **Szretter, K. J., et al.** 2010. The innate immune adaptor molecule MyD88 restricts West Nile virus replication and spread in neurons of the central nervous system. J. Virol. **84:**12125–12138.
58. **Szretter, K. J., et al.** 2009. The immune adaptor molecule SARM modulates tumor necrosis factor alpha production and microglia activation in the brainstem and restricts West Nile virus pathogenesis. J. Virol. **83:**9329–9338.
59. **Town, T., et al.** 2009. Toll-like receptor 7 mitigates lethal West Nile encephalitis via interleukin 23-dependent immune cell infiltration and homing. Immunity **30:**242–253.
60. **Wang, X., E. R. Hinson, and P. Cresswell.** 2007. The interferon-inducible protein viperin inhibits influenza virus release by perturbing lipid rafts. Cell Host Microbe **2:**96–105.
61. **Wang, Y., M. Lobigs, E. Lee, and A. Mullbacher.** 2003. CD8+ T cells mediate recovery and immunopathology in West Nile virus encephalitis. J. Virol. **77:**13323–13334.
62. **Wilkins, C., and M. Gale, Jr.** 2010. Recognition of viruses by cytoplasmic sensors. Curr. Opin. Immunol. **22:**41–47.
63. **Zhang, Y., C. W. Burke, K. D. Ryman, and W. B. Klimstra.** 2007. Identification and characterization of interferon-induced proteins that inhibit alphavirus replication. J. Virol. **81:**11246–11255.
64. **Zhu, H., J. P. Cong, and T. Shenk.** 1997. Use of differential display analysis to assess the effect of human cytomegalovirus infection on the accumulation of cellular RNAs: induction of interferon-responsive RNAs. Proc. Natl. Acad. Sci. U. S. A. **94:**13985–13990.